Supplementary Material

Materials and Methods

Instrumentation. Varian Inova 400 MHz and Inova 500 MHz NMR spectrometers were used to collect ^{1}H NMR spectra. ^{13}C NMR spectra were acquired using a Varian Mercury 300 MHz NMR spectrometer operating at 75 MHz. Evans' measurements of magnetic susceptibility and CEST data were acquired on Varian Inova 500 MHz NMR spectrometer. The temperature of the samples for ^{1}H NMR and CEST experiments was controlled with FTS Systems TC-84 Kinetics Air Jet Temperature Controller. A Thermo Scientific Orion 9826BN NMR micro pH electrode connected to a SympHony SB20 pH meter and the Orion 8115BNUWP Ross-ultra semi micro pH electrode connected to a Titrino 702 pH meter were used for pH measurements. ThermoFinnigan LCQ Advantage IonTrap LC/MS equipped with a Surveyor HPLC system was used to collect mass spectral data. A Beckman-Coulter DU 800 UV-vis Spectrophotometer equipped with a Peltier Temperature Controller was used to record absorbance spectra of $[Co(TPT)]^{2+}$ and $[Co(TPT)]^{3+}$ for characterization and for kinetic experiments of the reduction of Co(III) with sodium dithionite, and for the oxidation of Co(II) with oxygen. For the kinetic experiments, absorbance measurements were recorded every 60 seconds for 100-300 minutes.

The concentration of O_2 in solution was varied by changing its relative percentage with respect to total gas. The gases (O_2 and N_2) were mixed within a custom built gas mixing manifold, consisting of a matched pair of flow controllers (Gilmont Instruments, model: 77701– 2) connected to the gas cylinders.

Cyclic voltammograms were obtained using a Princeton Applied Research Model 263A Potentiostat/Galvanostat and PowerSuite software program. CHI 104 Glassy Carbon Disk working electrode from CH Instruments, Inc. (Austin, TX) was used. Standard Fisher Scientific Accumet Glass Body Ag/AgCl reference electrode was used, while a platinum wire served as a

counter electrode.   Potassium ferrocyanide was used as a standard for cyclic voltammetry measurements.

Determination of magnetic moment. The effective magnetic moment was calculated by using Evans' method.[1]   In a typical experiment, an oxygen-free solution of 8.0-20 mM $[Co(TPT)]^{2+}$ in deuterium oxide, pD 7.0, containing 5% *tert*-butanol by volume was placed in an NMR tube, while a reference solution of 5% *tert*-butanol (v/v) in deuterium oxide, pD 7.0, was placed into NMR tube insert.   All solutions of $[Co(TPT)]^{2+}$ were purged with argon and maintained under an argon atmosphere. The effective magnetic moment (μ_{eff}) was calculated at 298 K (T) by using the equations SI-SII given below. In these equations the mass susceptibility of solute (χ_g) was calculated by obtaining the observed frequency shift of the reference (Δf) in Hz, the spectrometer frequency (f) in Hz, the mass of the substance per cm^3 of the solution (m), and the mass susceptibility of deuterium oxide (χ_0= -0.6466 x 10^{-6} cm^3/g). The last term in eq. SI is neglected due to the minimal contribution to mass susceptibility of solute.   The molar susceptibility (χ_m) is the product of χ_g multiplied by the molecular weight of the $[Co(TPT)]Cl_2$ complex.[1] The reported value of the effective magnetic moment was obtained by averaging of three independent experiments.

$$\chi_g = (-3\Delta f)/(4\pi fm) + \chi_0 + [\chi_0 (d_0-d_s)]/m \qquad \textbf{eq. SI}$$

$$\mu_{eff} = 2.84 (\chi_m T)^{1/2} \qquad \textbf{eq. SII}$$

Dissociation of the $[Co(TPT)]^{2+}$ and $[Co(TPT)]^{3+}$ complex. ^{1}H NMR spectra (37 °C) were collected periodically over 24 hours using samples containing biologically relevant anions, Ca^{2+}, and Zn^{2+}, which were incubated at 37 °C under an argon atmosphere. Solutions contained 8 mM $[Co(TPT)]^{2+}$ or $[Co(TPT)]^{3+}$ complex, 100 mM NaCl, 0.40 mM Na_2HPO_4 , 25.0 mM K_2CO_3, and 10.0 mM 3-(trimethylsilyl)propionic acid sodium salt (TMSP) as an internal [1]H

NMR standard in deuterium oxide, pD 7.5. The ^{1}H NMR spectra were obtained after 0.5 h, 12 h, 18 h, and 24 h of incubation at 37 ^{o}C (Figure S6). Integrated intensities of the aromatic protons with chemical shifts δ = 14.4 and 82.6 ppm (37 ^{o}C) were compared to integrated intensities of methyl protons of TMSP for the quantification of $[Co(TPT)]^{2+}$ dissociation. Integrated resonance intensities of diamagnetic protons of $[Co(TPT)]^{3+}$ were taken into account when the total concentration of complex was calculated. In these experiments on $[Co(TPT)]^{2+}$ dissociation, the concentration of $[Co(TPT)]^{3+}$ contributed less than 5% of the total concentration of complex after 24 h of incubation under argon.

CEST experiments. In general, CEST data was acquired with a pre-saturation pulse power (B_1) of 1093 Hz applied for 3 seconds. Most of the CEST data was obtained at 37 ^{o}C. Data were acquired in 1 ppm increments and were plotted as normalized water intensity against frequency offset to produce a CEST spectrum. Samples containing 8 mM metal complex were prepared from freshly synthesized $[Co(TPT)]^{2+}$, or from $[Co(TPT)]^{3+}$ with subsequent addition of reducing aliquots of sodium dithionite, or L-cysteine. Solutions also contained 20.0-40.0 mM of appropriate buffers of desired pH and 100-200 mM NaCl. The higher concentrations of buffer (40.0 mM) and salt (200 mM) were used to ensure that pH doesn't change upon addition of reducing agents, anions, and cations during titration experiments. Samples for the CEST experiments in serum were prepared by mixing of $[Co(TPT)]^{2+}$ (pH 7.0) in water with a reconstituted aqueous solution of normal rabbit serum at adjusted pH of 7.0. An NMR tube insert filled with DMSO-d_6 was used to lock the signal on NMR spectrometer. The pH dependence of CEST was measured in the range of pH 5.4-8.1 using 40 mM MES, HEPES, or CHES with 200 mM NaCl. All CEST samples were purged with argon for 15 minutes prior to the addition of $[Co(TPT)]Cl_2$, and they were kept under inert atmosphere during the course of the

experiments. For CEST experiments, the reconstituted rabbit serum in water was adjusted to pH 7.0. After purging of the solution of serum with argon in an NMR tube for 15 min, an aliquot of an argon saturated stock solution of $[Co(TPT)]^{2+}$ in water, pH 7.0, was added via gas-tight syringe. The NMR tube was additionally purged with argon for 5 min, equipped with an insert containing DMSO-d_6, and sealed to prevent contact with air.

Exchange rate constants. The exchange rate constants were calculated by using a previously reported procedure.[2] The magnetization of the on-resonance (M_z) and off-resonance (M_o) were acquired at different pre-saturation pulse powers between 350-1090 Hz applied for 4 seconds. To calculate the exchange rate constant (k_b), the x-intercept ($-1/ k_b^2$) was obtained from the plot of $M_z/(M_o-M_z)$ against $1/\omega_1^2$ (ω_1 in rad/s) (Figure S7). Samples contained 16.0 mM $[Co(TPT)]Cl_2$, 200 mM NaCl, and 40.0 mM MES or HEPES at pH 6.4-7.5. Measurements were carried out at 37 °C.

Extinction coefficient of $[Co(TPT)]^{3+}$. A concentration of $[Co(TPT)]^{3+}$ stock solution in D_2O containing 100 mM NaCl, pH 7.0, was calibrated by ^1H NMR experiments using 10.0 mM TMSP as an external standard. An extinction coefficient of 404 ± 10 $M^{-1}cm^{-1}$ was obtained for the characteristic absorbance band of $[Co(TPT)]^{3+}$ at $\lambda = 485$ nm using a serial dilution method.

Kinetic measurements. Pseudo-first order reaction conditions were used for measuring rate constants for the reaction of 0.60 mM $[Co(TPT)]^{3+}$ and sodium dithionite (1.90-6.40 mM). Solutions of 0.60 mM $[Co(TPT)]^{3+}$ in 0.20 M NaCl and 40.0 mM HEPES, pH 7.0, were purged with argon in a one cm path-length quartz cuvette equipped with a gas-tight septum. Aliquots of argon-purged solutions of $Na_2S_2O_4$ in 0.20 M NaCl, pH 7.0, were added to the UV-vis cuvette *via* a gas-tight syringe. The reduction of $[Co(TPT)]^{3+}$ to $[Co(TPT)]^{2+}$ was monitored over a period of 100 min by following the absorbance decrease at $\lambda = 485$ nm (Figure S12). The decay

traces were fit to single exponential decays to give pseudo-first order rate constants. The first-order rate constants were plotted as a function of $Na_2S_2O_4$ concentration. The linear fit of the data gave a bimolecular rate constant, $k_{bi} = 0.24 \ M^{-1}s^{-1}$, for the reaction between $[Co(TPT)]^{3+}$ and $Na_2S_2O_4$ (Figure S13).

Pseudo-first order rate constants for the reaction of 70 µM $[Co(TPT)]^{2+}$ at various pO_2 were obtained in aqueous solutions containing 0.20 M NaCl and 40.0 mM HEPES, pH 7.1, using a five cm path-length quartz cuvette equipped with a gas-tight septum. The solutions were equilibrated by gentle purging with desired O_2/N_2 mixtures for 40 min prior to the addition of an aliquot of $[Co(TPT)]^{2+}$ in the minimal volume of solvent. The $[Co(TPT)]^{2+}$ stock solution was kept under argon atmosphere prior to the addition to the UV-vis cuvette *via* a gas-tight syringe. The oxidation process of $[Co(TPT)]^{2+}$ was monitored over a period of 180-300 min, depending on O_2 concentration, by following the absorbance increase at $\lambda = 485$ nm due to the formation of $[Co(TPT)]^{3+}$ (Figure S14). Absorbance kinetic traces were fit to a single exponential dependence yielding pseudo-first order rate constants. The first-order rate constants were plotted as a function of O_2 concentration. The linear fit of the data gave a bimolecular rate constant, $k_{bi} = 0.43 \ M^{-1}s^{-1}$, for the reaction between $[Co(TPT)]^{2+}$ and O_2 (Figure 4).

PARACEST imaging. CEST images were acquired on a 4.7 Tesla preclinical MR scanner using a 35 mm radiofrequency coil and the ParaVision 3.0.2 research platform (Bruker Biospin, Billerica, MA). A pair of gradient-echo MR images were acquired at 37 °C with a pre-saturation pulse train comprised of five 1 second Gauss pulses (12 µT , 200 µs interpulse delay) applied symmetrically about the bulk water resonance (+/-135 ppm). Other pertinent acquisition parameters include: echo time/repetition time = 2.1/5010 ms, flip angle = 90 deg, acquisition matrix = 160x160, slice thickness = 2 mm, field of view = 32 x 32mm, averages = 1.

To determine the CEST effect, each image was normalized to the signal intensity of the buffer and salt-only phantom and the normalized image intensity of each phantom was sampled using commercially available software (Analyze 7.0, AnalyzeDirect Inc., Overland Park, KS). The percent loss of signal due to PARACEST exchange was calculated using the equation:

% CEST = 1 - SI_{on}/SI_{off},   **eq. SIII**

where SI_{on} and SI_{off} are the image intensities of each sample acquired with on-resonance and off-resonance pre-saturation pulses, respectively. To create the CEST image (Figure 3-I), raw k-space data was zero-filled to a 512 x 512 matrix, reconstructed to spatial domain, filtered with a spatial low-pass filter (kernel size: 11 x 11) to improve signal-to-noise, and then normalized by image intensity of the buffer and salt-only phantom. The % CEST effect was calculated pixel-by-pixel using the normalized on/off resonance image pair in MATLAB (MathWorks, Natick, MA). Phantoms in the CEST image were isolated using binary masking techniques, and a "hot-iron" pseudocolor lookup table was applied to enhance perceptual contrast between samples.

T_1/T_2 Relaxivity. Samples of 2.0 mM, 4.0 mM, and 8.0 mM of [Co(TPT)]Cl_2 in 100 mM NaCl and 20.0 mM HEPES, pH 7.0, were used for T_1/T_2 relaxivity measurements. T_1/T_2 relaxivity values were determined on a 4.7 Tesla MRI system. T_1 relaxation rate constants of solutions of the complex made by serial dilutions were measured using an inversion-recovery TrueFISP acquisition with the following parameters: TE/TR=1.5/3.0 ms, flip angle=30°, inv. repetition time=10 s, segments=8, frames=100. T_2 relaxation rate constants were measured using a multi-echo, Carr-Purcell-Meiboom-Gill (CPMG) spin-echo sequence with a fixed TR of 3000 ms and TE times ranging from 20-1200 ms in 20 ms increments (60 echoes). The relaxation rate constant of each sample calculated using non-linear regression analysis routines developed in

MATLAB and relaxivities were then calculated by linear regression (concentration vs. relaxation rate constant). Results are reported in Figure S11.

Cyclic Voltammetry. Cyclic voltammetry experiments showed a reversible oxidation for 1.7 mM [Co(TPT)]$^{2+}$ at 1.00 M KCl under argon at 25 $^{\circ}$C (Figure S10). The external ferrocyanide standard with $E^{\circ}(Fe^{III}/Fe^{II}) = 303 \pm 10$ mV vs. NHE contained 1.0 mM K$_4$Fe(CN)$_6$ and 1.00 M KCl under argon. The redox potential of the complex was calculated based on a NHE reference using eq. SIV:

$$E^{\circ} \text{ (vs. NHE)} = E^{\circ} \text{ (vs. Ag/AgCl)} + 167 \text{ mV}, \qquad \textbf{eq. SIV}$$

Materials. All solvents and reagents were reagent grade, and they were used as received without additional purification. 1,4,7-Triazacyclononane (TACN) was purchased from TCI America (Portland, OR), and 3-(chloromethyl)-1*H*-pyrazole hydrochloride was purchased from Accela ChemBio Inc. (San Diego, CA). *N,N*-Diisopropylethylamine (DIPEA), 1,8-diazabicycloundec-7-ene (DBU), *L*-ascorbic acid and normal rabbit serum were obtained from Sigma-Aldrich (St. Louis, MO). Cobalt(II) chloride hexahydrate, sodium dithionite, and sodium peroxydisulfate were received from Alfa Aesar (Ward Hill, MA). Basic alumina (50-200 μm) was purchased from Dynamic Adsorbents Inc. (Norcross, GA).

Synthetic Methods
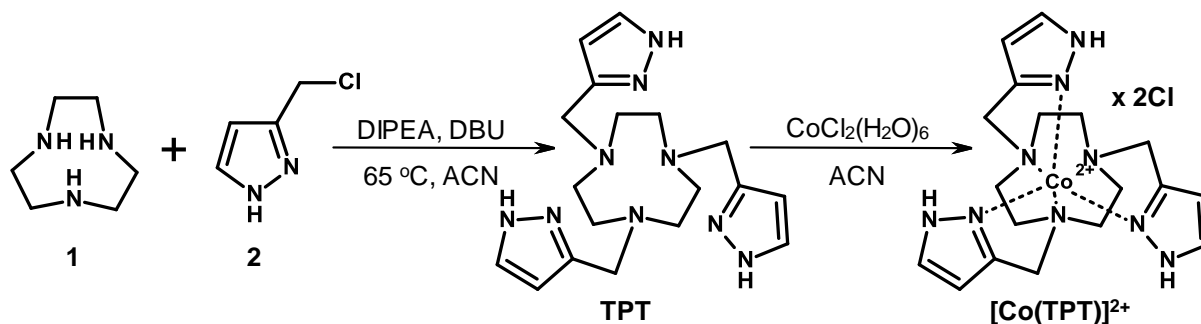
Scheme S1. Synthesis of TPT ligand and [Co(TPT)]$^{2+}$ complex.

Synthesis of 1,4,7-tris(pyrazol-3-ylmethyl)-1,4,7-triazacyclononane (TPT). 3-(Chloro-methyl)-1H-pyrazole hydrochloride (0.58 g, 3.8 mmol, 3 equiv.) was added in one portion to an argon-purged solution of TACN (0.16 g, 1.3 mmol) and 1.4 mL of DIPEA (1.1 g, 8.2 mmol, 6.5 equiv.) in 65 mL of acetonitrile (ACN) heated at 70 ^{o}C. After stirring at 70 ^{o}C for 45 min, a portion of DBU (0.77 g, 5.1 mmol, 4 equiv in 0.75 mL) was added to the reaction mixture. The reaction mixture was further stirred at 60 ^{o}C under argon for 8 h. Solvent (ACN) was removed *in vacuo,* producing a yellow solid. The solid was redissolved in a minimal volume of methanol, and diethyl ether was added drop-wise until a white cloudy precipitate was formed. This precipitate turned into oil after placing the sample at -20 ^{o}C for 3 h. The supernatant, which contained the product, was isolated upon decantation, and the solvent was removed *in vacuo* to produce a yellowish residue. This residue was subject to column chromatography using ca. 100 mL of basic Al$_2$O$_3$ packed with 2% methanol in methylene chloride. The product was eluted by using a solvent gradient containing 2% to 15% of methanol in methylene chloride. Yield: 0.24 g, 51%. ^{1}H NMR, 500 MHz (CDCl$_3$, ppm): δ = 7.52 d (3H, Ar, J = 2 Hz), 6.11 d (3H, Ar, J = 2 Hz), 3.76 s (6H, 3xCH$_2$), 3.48 s (3xNH), 2.67 m (12H,

6xCH$_2$). ^{13}C NMR, 75 MHz (CD$_3$OD, ppm): δ = 146.92, 134.78, 105.92, 54.56, 54.11 (Figure S15). ESI-MS (m/z): [M+H]$^+$, calculated: 370.2, found: 370.3.

Synthesis of [Co(TPT)]$^{2+}$. In a representative procedure, TPT (40 mg, 0.11 mmol) was placed in the tube with 1.1 mL of acetonitrile. After purging the solvent with argon, CoCl$_2$(H$_2$O)$_6$ (25 mg, 0.11 mmol) was added. The reaction mixture was again purged with argon while stirring. This reaction mixture was sonicated for 10 min followed by stirring for 20 min. The sonication/stirring was repeated five times. A sky-blue flaky precipitate of [Co(TPT)]Cl$_2$ was formed upon sonication, while the dark-blue crystalline CoCl$_2$(H$_2$O)$_6$ disappeared. After sonication for a total period of 60 min, the reaction mixture was stirred under argon at r.t. After 8 h the reaction mixture was centrifuged, and the blue supernatant was decanted. The sky-blue solid was washed with 200 µL of acetonitrile. The mixture was centrifuged, and the slightly blue supernatant was decanted affording [Co(TPT)]Cl$_2$ as a blue solid. Yield: 36 mg, 0.07 mmol, 67%. ^{1}H NMR of the product in argon-purged D$_2$O, pD 5.2, indicated that >95% of complex was present in the paramagnetic Co(II) state, while additional diamagnetic signals corresponded to <5% of complex in Co(III) form. ^{1}H NMR, 500 MHz (D$_2$O, pD 5.2, ppm) at 25 ^{o}C: δ = 210.06 s br. (3H), 195.64 s br. (3H), 133.80 s br. (3H), 100.13 s br. (3H), 82.61 s (3H, Ar), 14.39 s (3H, Ar), -22.32 s br. (3H), -102.86 s br. (3H). This product was further characterized in both Co(II) and Co(III) forms.

Synthesis of [Co(TPT)]Cl$_3$. The Co(III) complex was prepared by oxidation of the Co(II) complex. In a typical preparation, [Co(TPT)]Cl$_2$ (15 mg, 30 µM) was dissolved in 0.8 mL of a solution containing 100 mM NaCl in D$_2$O. The initial solution pD of 4.5 was adjusted to neutral by addition of 4% NaOD solution in D$_2$O. Upon stirring under air, the color of the solution turned tea-red. The solution was maintained at a pD of 6.8-7.2 by adding aliquots of 4%

NaOD in D_2O every 15 min for 4 h. The reaction mixture was stirred under air for 8 h, and the pD was adjusted to neutral several times over the course of the reaction. The completion of oxidation was confirmed by ^{1}H NMR in D_2O, pD 7.0. The solvent was removed by lyophilization, producing a red powder. ^{1}H NMR, 500 MHz (D_2O, pD 7.0, ppm): δ = 7.66 d (3H, Ar, J = 2 Hz), 6.46 d (3H, Ar, J = 2 Hz), 4.03 dt (6H, NC$\underline{H}_2$Ar), 3.88 ddd (3H, NC$\underline{H}^{ax}$HCH$_2$, axial), 3.41 dd (3H, NC$\underline{H}^{eq}$HCH$_2$, equatorial), 2.88 dd (3H, NC$\underline{H}^{eq}$HCH$_2$, equatorial), 2.30 ddd (3H, NC$\underline{H}^{ax}$HCH$_2$, axial) (Figure S16). Assignments of ring protons are based on comparison to reported complexes.[3] ^{13}C NMR, 75 MHz (D_2O, ppm): δ = 154.84, 141.17, 105.84, 63.94, 63.15, 62.58. ESI-MS (m/z): [M-2H$^+$]$^+$, calculated: 426.2, found: 426.2 (100%); [2*(M-3H$^+$)+H$^+$]$^+$, calculated: 851.3, found: 851.2 (85%); [3*(M-3H$^+$)+H$^+$]$^+$, calculated: 1276.5, found: 1276.2 (65%).
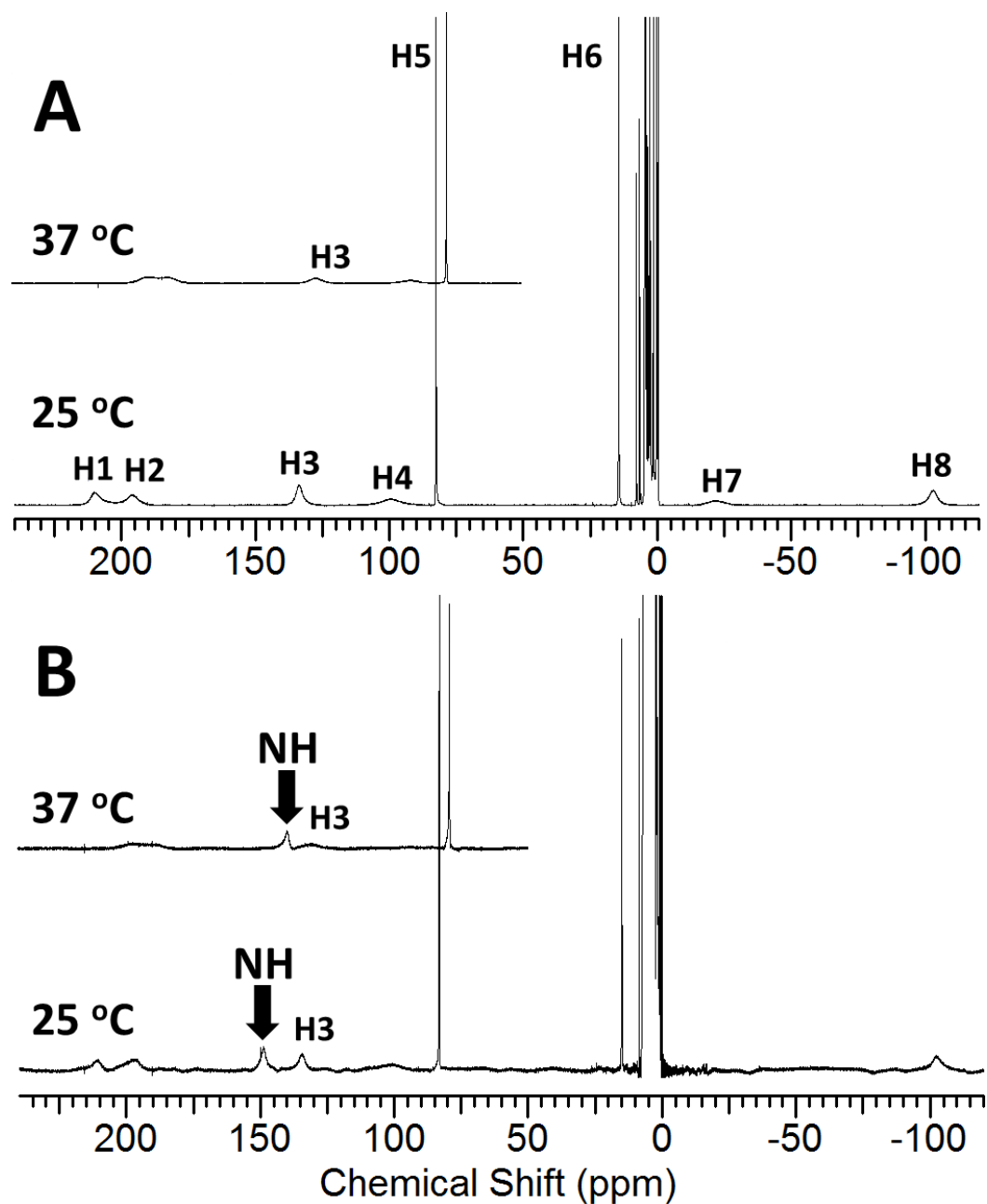
Figure S1. ^{1}H NMR spectra of $[Co(TPT)]^{2+}$ in D_2O, 100 mM NaCl, pD 5.2 (A) and in H_2O, 100 mM NaCl, pH 5.0 (B) at 25 ^{o}C. Inserts show regions of the spectra (50-240 ppm) obtained at 37 ^{o}C. Proton resonances H5 and H6 are tentatively assigned to aromatic CH protons of pyrazole, while signal from the exchangeable protons at 149 ppm, 25 ^{o}C (140 ppm, 37 ^{o}C) is tentatively assigned to NH protons of pyrazole ring. The diamagnetic region consists of resonances arising from the complex in Co(III) state.
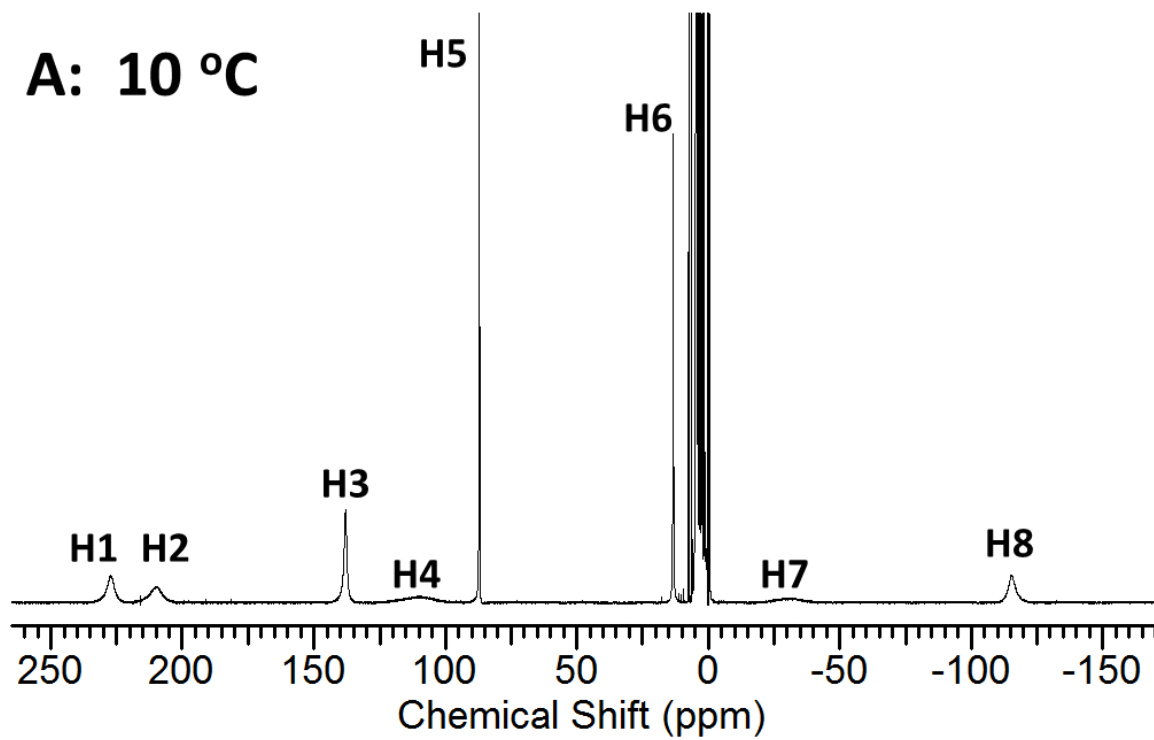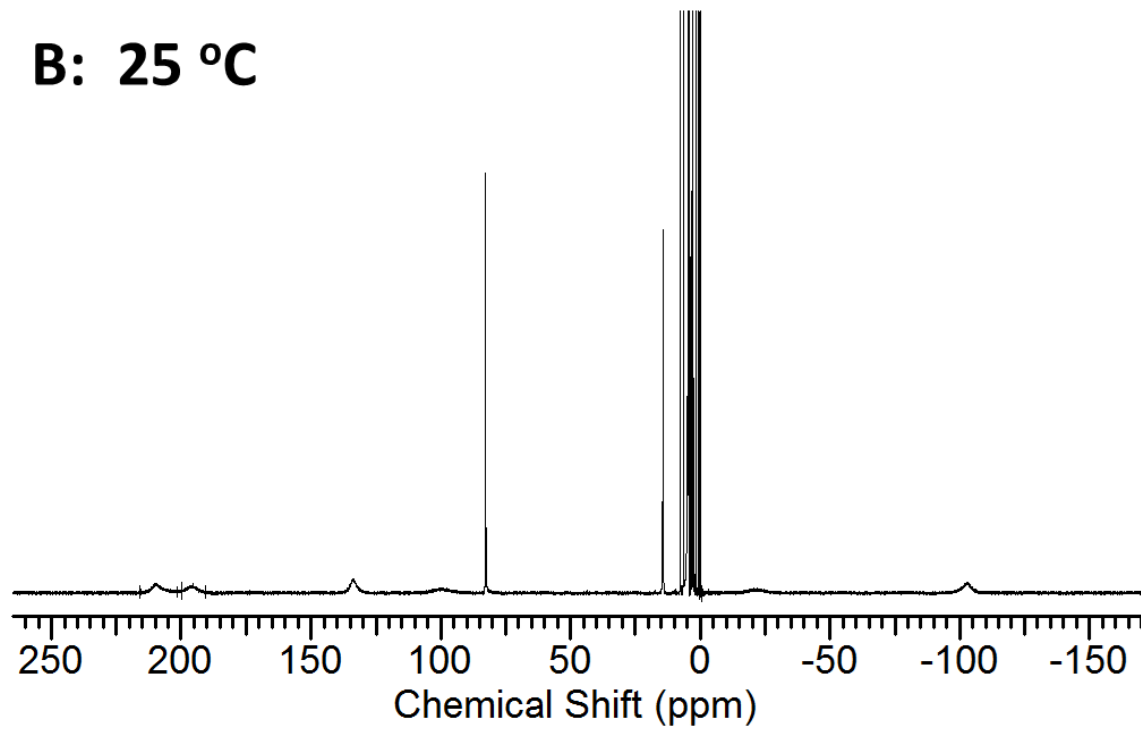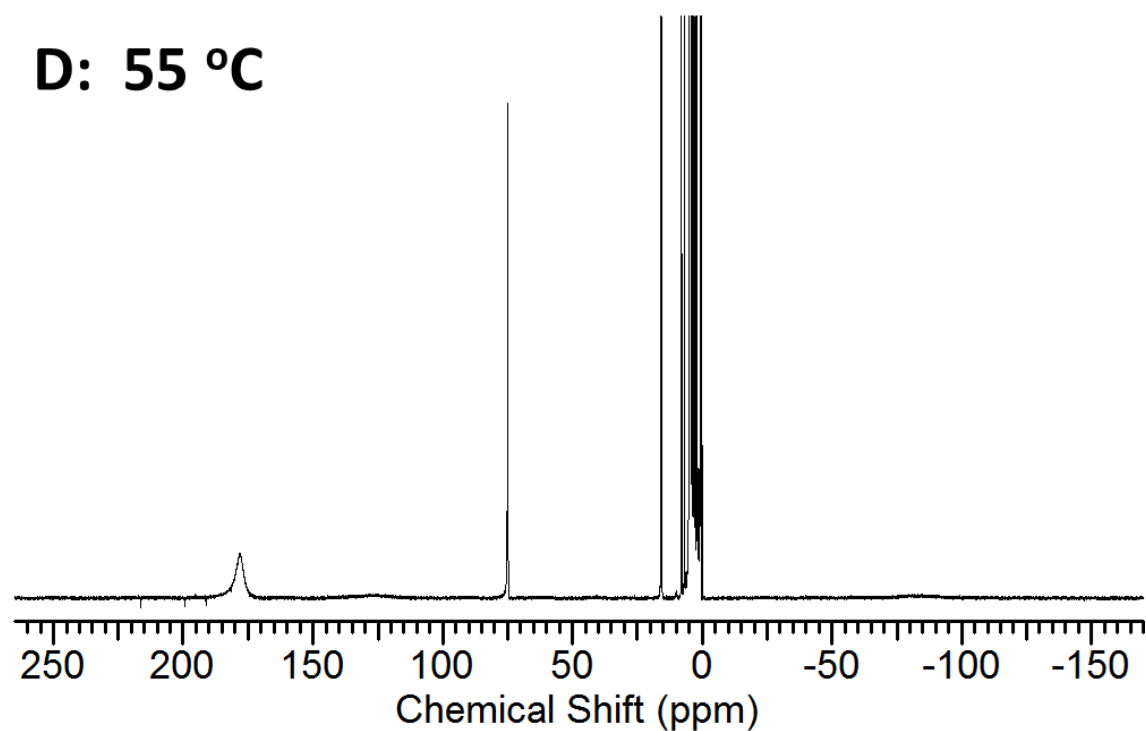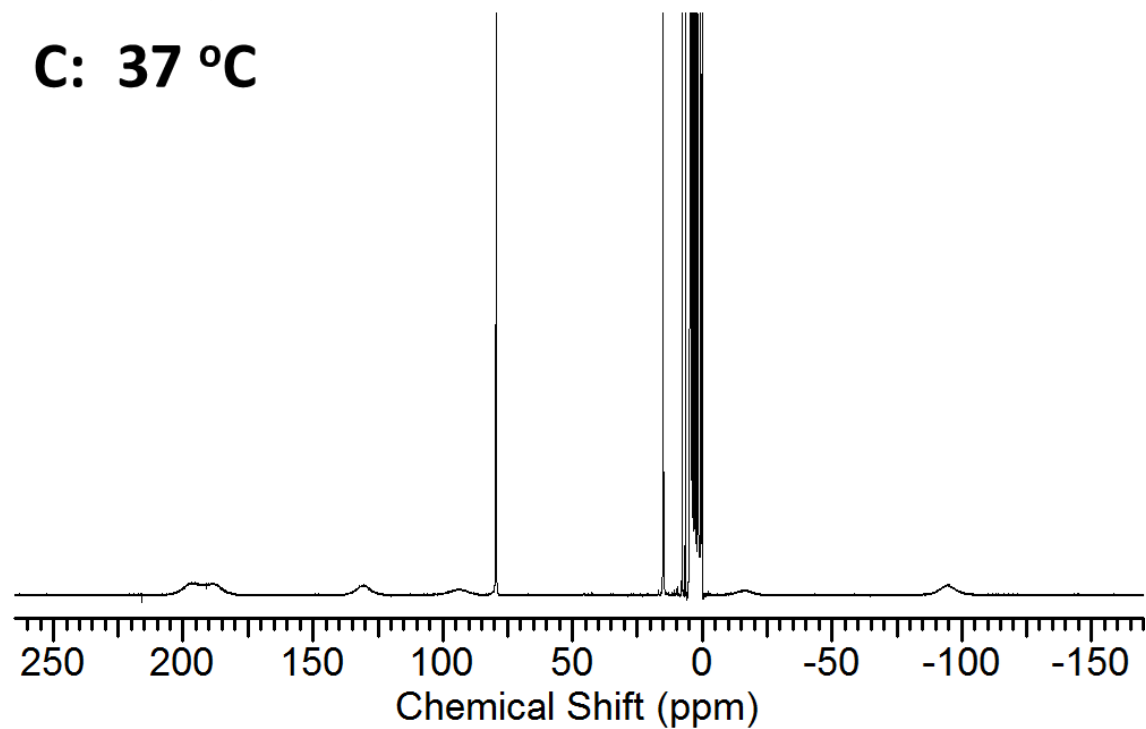
Figure S2. Temperature dependence (10 °C – 55 °C) of ^{1}H NMR spectra of $[Co(TPT)]^{2+}$ in D_2O, pD 7.30, 100 mM NaCl. At lower temperatures of 10 – 37 °C, eight resonances of non-exchangeable protons **H1-H8** are distinguished, as labeled in spectrum A (10 °C). Resonances in the diamagnetic region arise from the Co(III) complex.
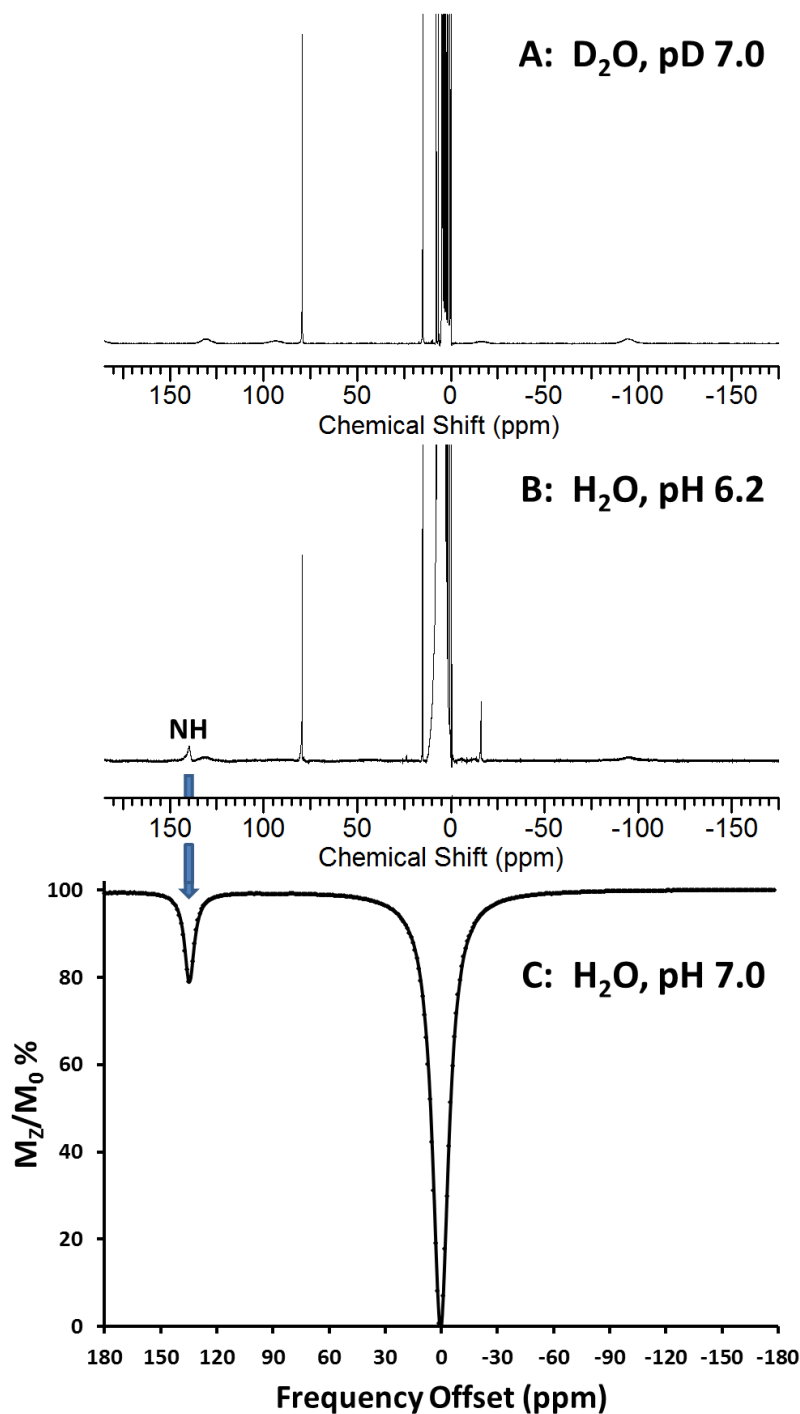
Figure S3. ^{1}H NMR spectra at 37 °C of [Co(TPT)]$^{2+}$ in D$_2$O, 100 mM NaCl, pD 7.0 (A) and in H$_2$O, 100 mM NaCl, pH 6.2 (B) in comparison to CEST spectrum (3 s, B$_1$ = 24 μT) of 8.0 mM [Co(TPT)]Cl$_2$ in aqueous solution of 100 mM NaCl, 20.0 mM HEPES, pH 7.0 at 37 °C (C). Arrow shows that the chemical shift of the exchangeable proton resonance corresponds to that of the CEST peak. Note that in the CEST spectrum, the water peak is set to 0 ppm. Exchangeable protons are tentatively assigned to NH of pyrazole rings.
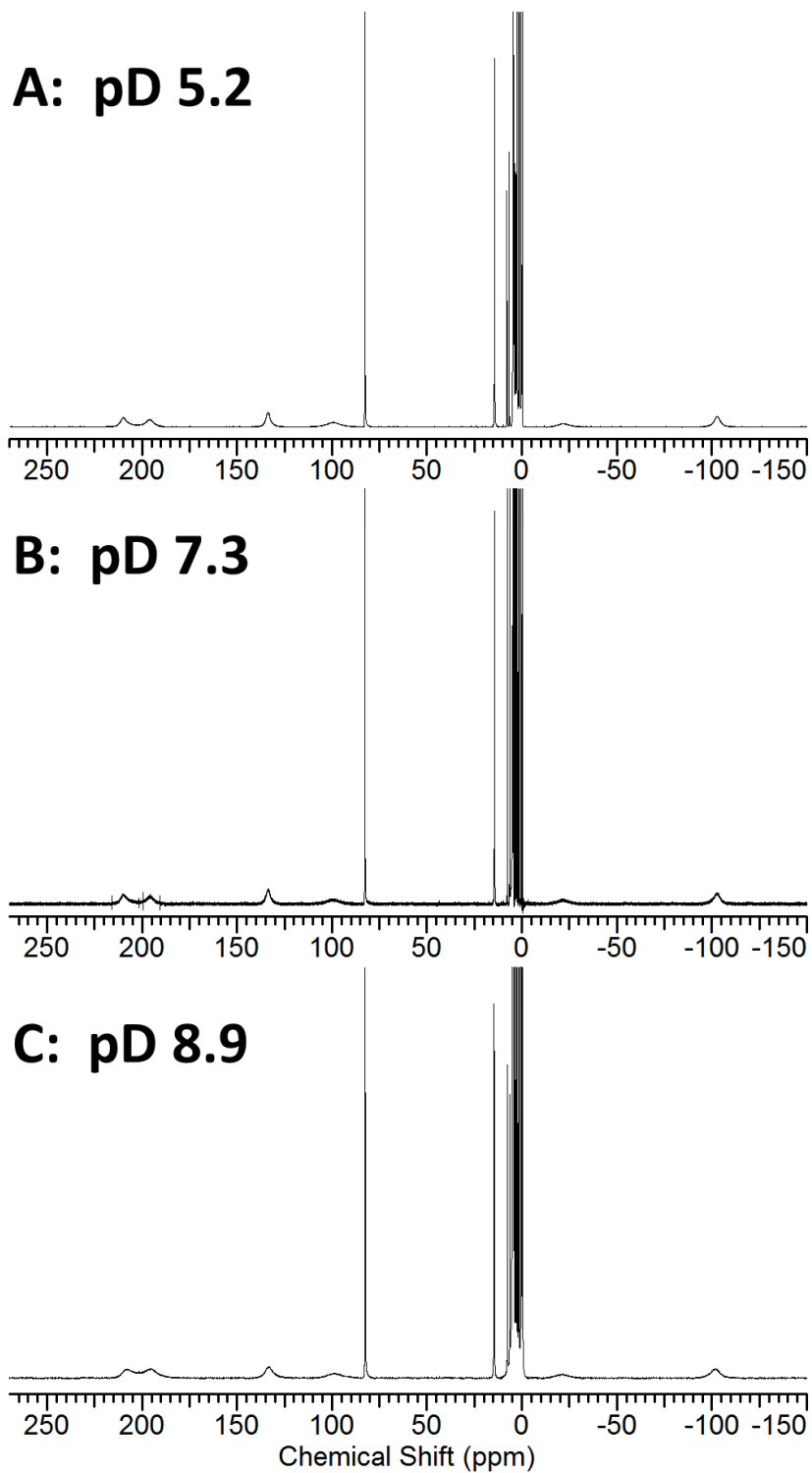
Figure S4. pH (pD) dependence of ^{1}H NMR spectra of $[Co(TPT)]^{2+}$ at 25 ^{o}C in D_2O containing 100 mM NaCl at pD 5.2 (A), pD 7.3 (B), and pD 8.9(C). Resonances in the diamagnetic region arise from the complex in the Co(III) state.

A). No reducing agent.

0% [Co(TPT)]$^{2+}$
100% [Co(TPT)]$^{3+}$
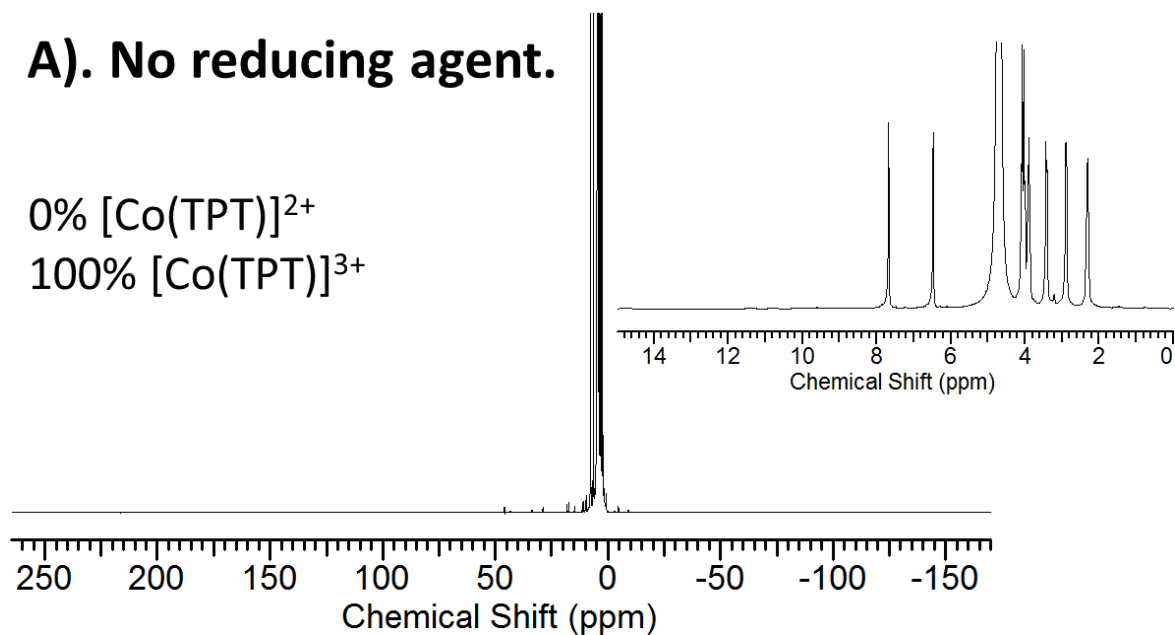
B). 0.25 equiv. Na$_2$S$_2$O$_4$

37% [Co(TPT)]$^{2+}$
63% [Co(TPT)]$^{3+}$

C). 0.5 equiv. Na$_2$S$_2$O$_4$

68% [Co(TPT)]$^{2+}$
32% [Co(TPT)]$^{3+}$

D). 0.75 equiv. Na$_2$S$_2$O$_4$
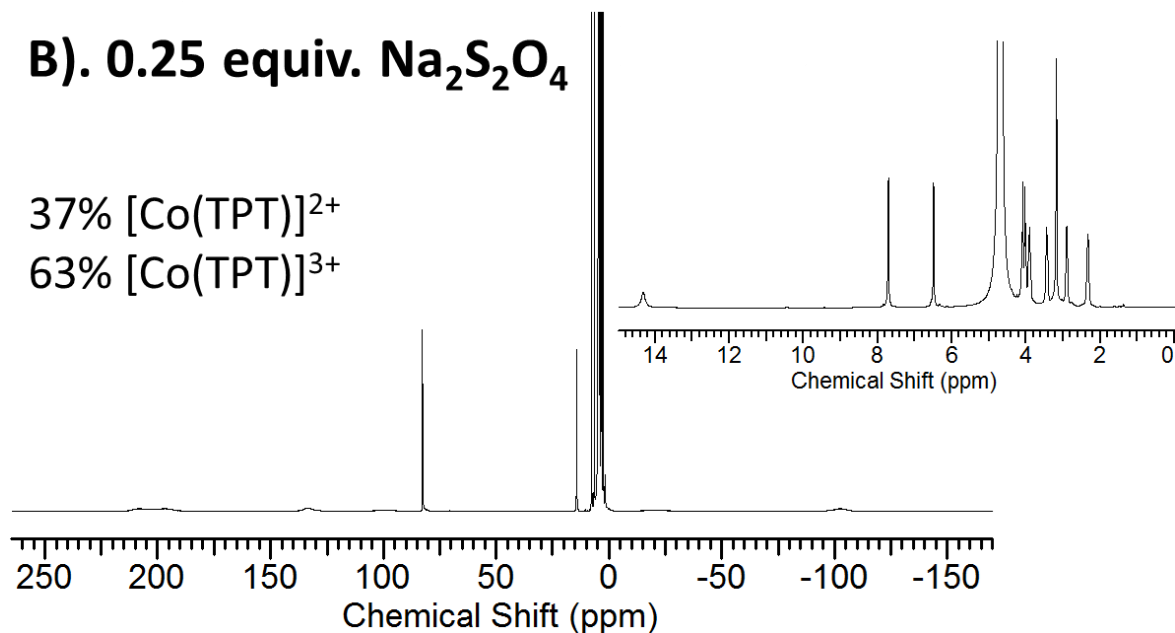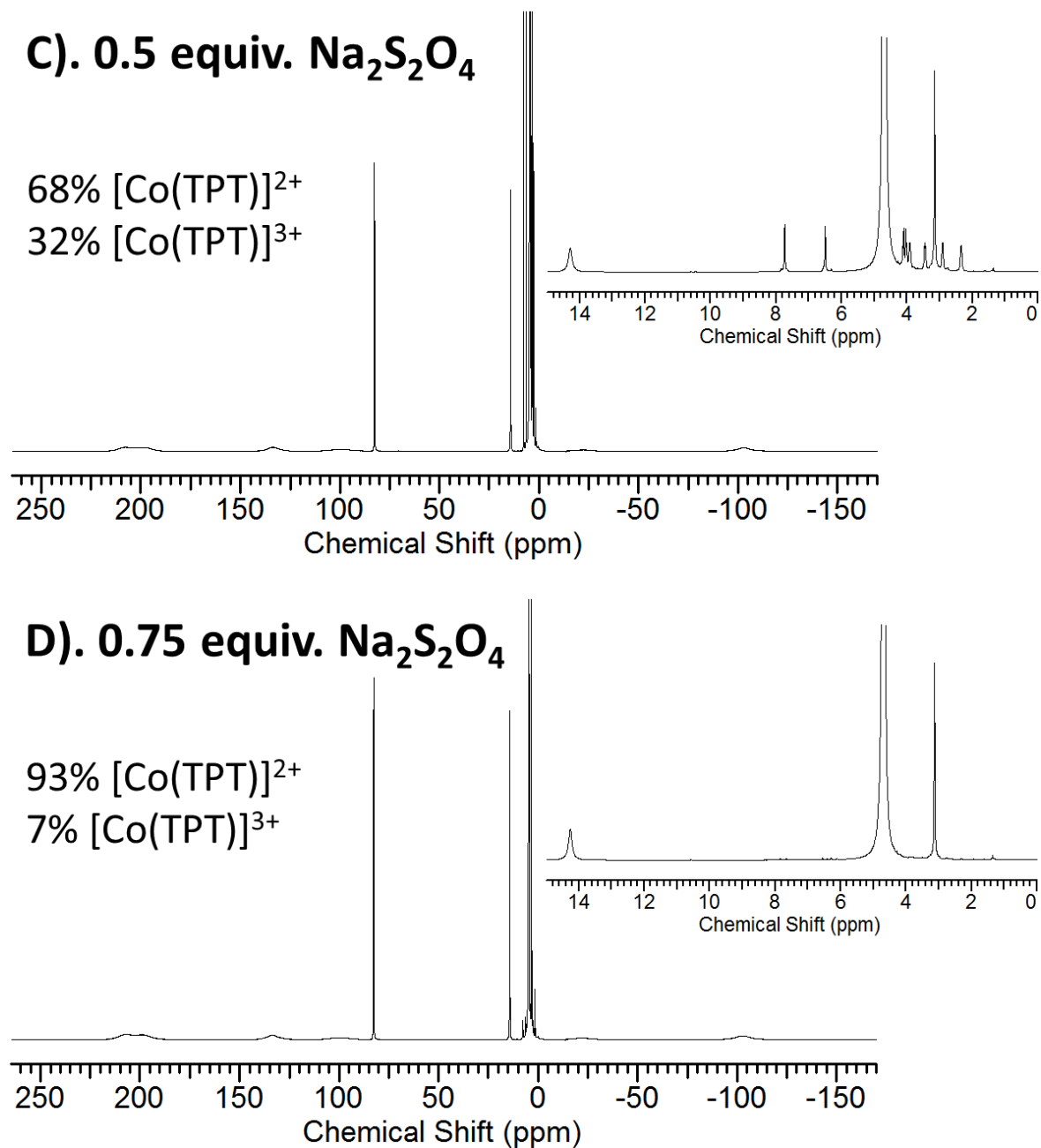
93% [Co(TPT)]$^{2+}$
7% [Co(TPT)]$^{3+}$

Figure S5. Reduction of 30 mM [Co(TPT)]$^{3+}$ in D$_2$O (pD 7.10, 100 mM NaCl) with 0.25, 0.50, and 0.75 equiv. of Na$_2$S$_2$O$_4$. Near complete reduction to [Co(TPT)]$^{2+}$ is observed at 0.75 equiv. of Na$_2$S$_2$O$_4$. Insert shows diamagnetic region together with paramagnetic peak at δ = 14.5 ppm. Intensity of the resonance at 14.5 ppm increases with addition of Na$_2$S$_2$O$_4$, while diamagnetic signals disappear.

A: 30 min

15   10   5   0
Chemical Shift (ppm)

250   200   150   100   50   0   -50   -100   -150
Chemical Shift (ppm)

* * **

B: 12 h

15   10   5   0
Chemical Shift (ppm)

250   200   150   100   50   0   -50   -100   -150
Chemical Shift (ppm)

* * **
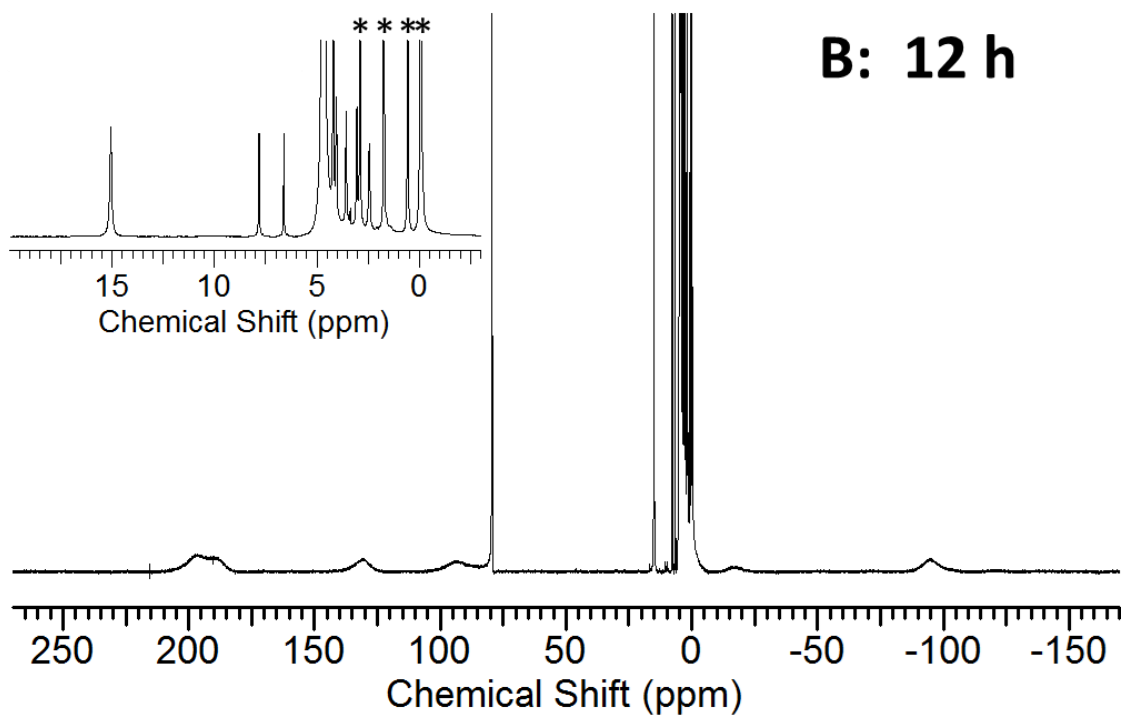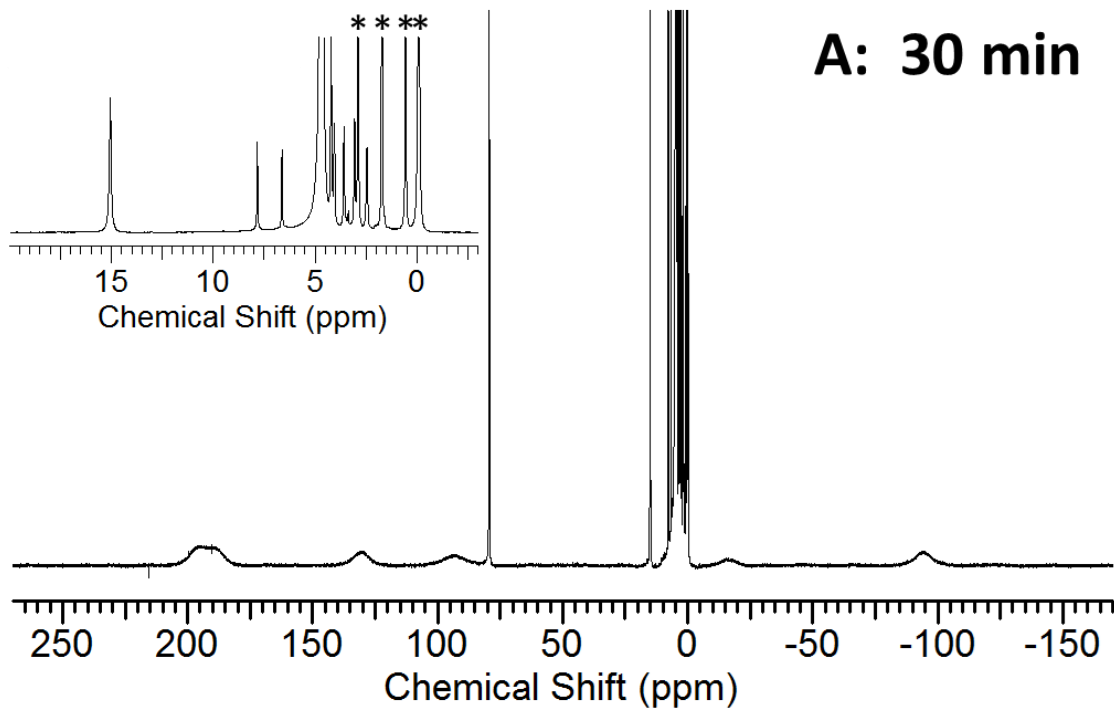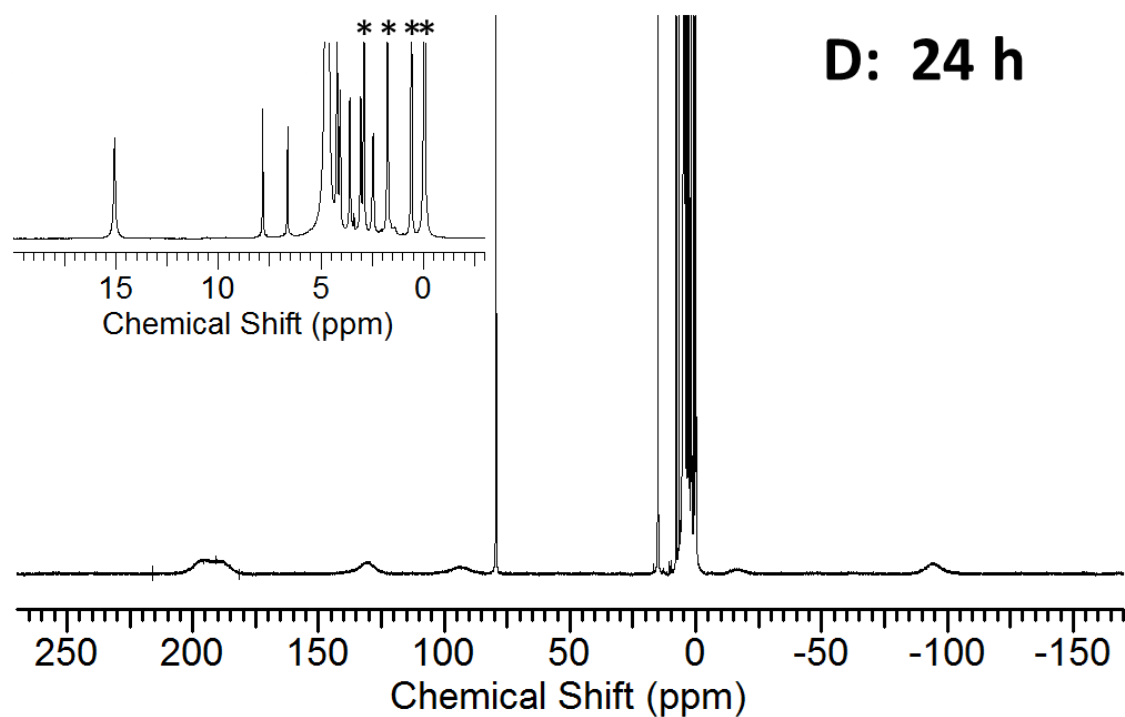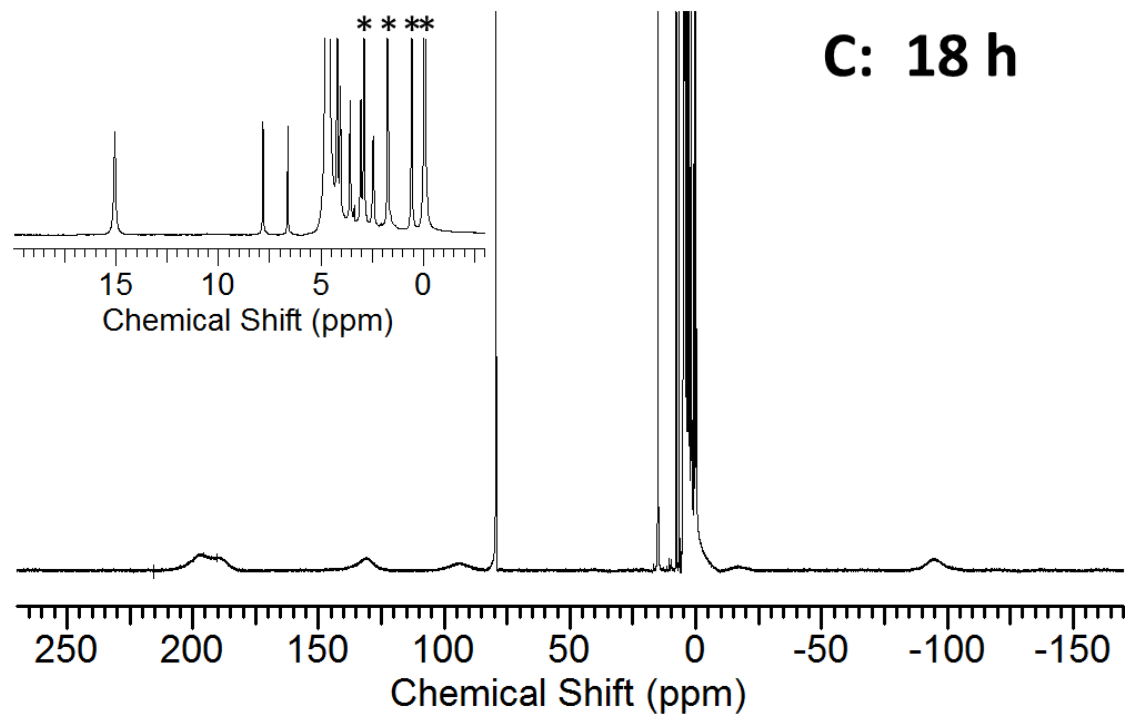
Figure S6. ^{1}H NMR spectra of 8.0 mM [Co(TPT)]$^{2+}$ incubated at 37 $^{\circ}$C in D$_2$O solution containing 0.40 mM K$_3$PO$_4$, 25.0 mM K$_2$CO$_3$, and 100 mM NaCl, pD 7.5, for 0.5, 12, 18, and 24 h. Insert shows diamagnetic region with one paramagnetically shifted peak at δ = 15 ppm and peaks from the Co(III) complex. Asterisks represent signals from 10 mM TMSP.

Table S1. Dissociation of the complexes in the presence anions and cations.

		Ca^{2+}	Zn^{2+}	$PO_4^{3-}/CO_3^{2-}/Cl^-$
	6h h	0	0	0
$[Co(TPT)]^{2+}$	12 h	2*	4*	0
	24 h	2*	5*	0
	6h h	0	0	0
$[Co(TPT)]^{3+}$	12 h	0	2*	0
	24 h	0	2*	0

Samples contained 5 mM cobalt complex and either 1) 5 mM Ca^{2+} at pH 7.20, 2) 5 mM Zn^{2+} at pH 6.50, or 3) 0.40 mM phosphate, 25 mM carbonate and 100 mM NaCl at pD of 7.50. All samples were incubated at 37 °C and contained 5-10 mM TMSP as a standard for quantitative analysis. *Detection limits for analysis of complex dissociation by ^1H NMR spectroscopy are approximately 5%, suggesting that there is little or no dissociation of the complexes.
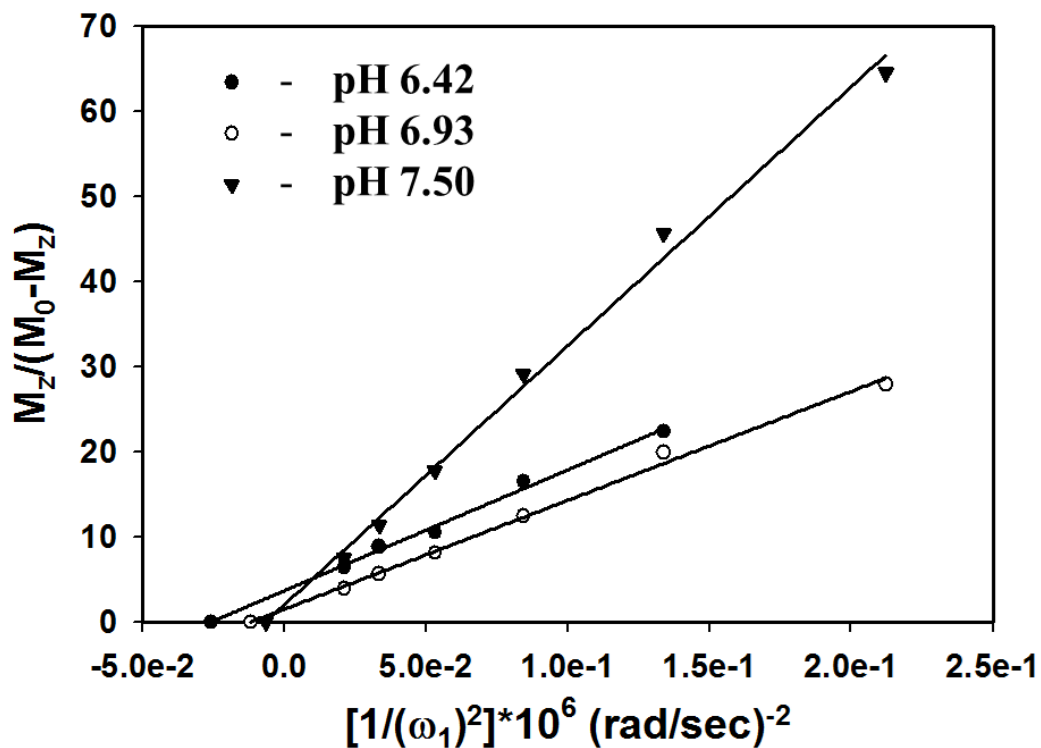
Figure S7. Determination of the exchange rate constants (k_b) at pH 6.42, pH 6.93, and pH 7.50 at 37 °C. Data points (except x-intercept points) correspond to the CEST signal intensity at 135 ppm obtained at various pre-saturation pulse powers of 350-1090 Hz applied for 4 seconds. Solid lines represent the linear fit of the data for each sample. The x-intercept values are obtained by extrapolation of linear fits. Samples contained 16.0 mM $[Co(TPT)]^{2+}$, 200 mM NaCl, and 40.0 mM MES or HEPES.
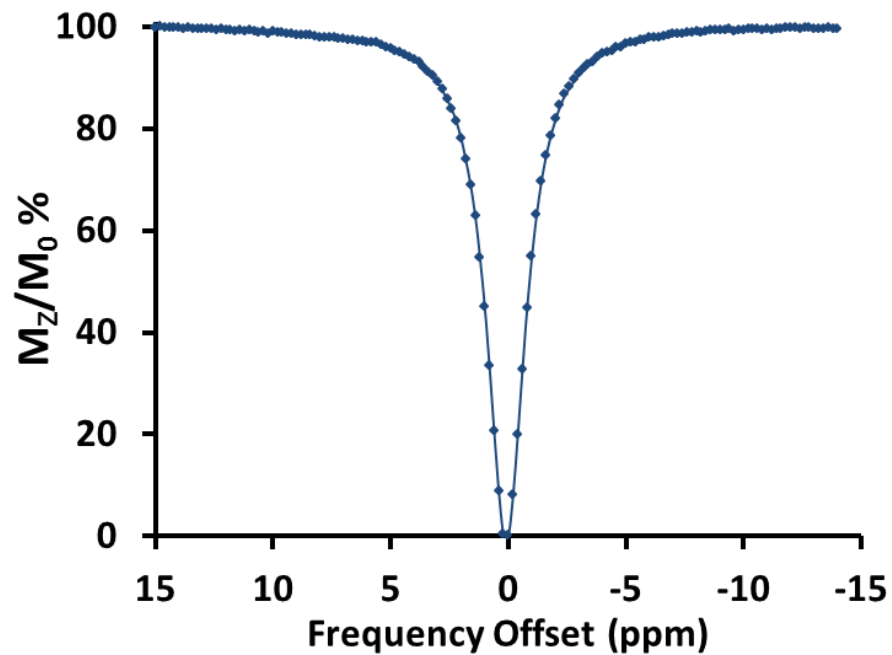
Figure S8. Z-spectrum obtained for 12 mM $[Co(TPT)]^{3+}$ in 200 mM NaCl, 40 mM HEPES, pH 7.1 at 37 $^{\circ}$C, indicating absence of diaCEST effect under biologically relevant conditions. RF pre-saturation applied for 3 seconds, $B_1 = 5.6$ μT at 37 °C.
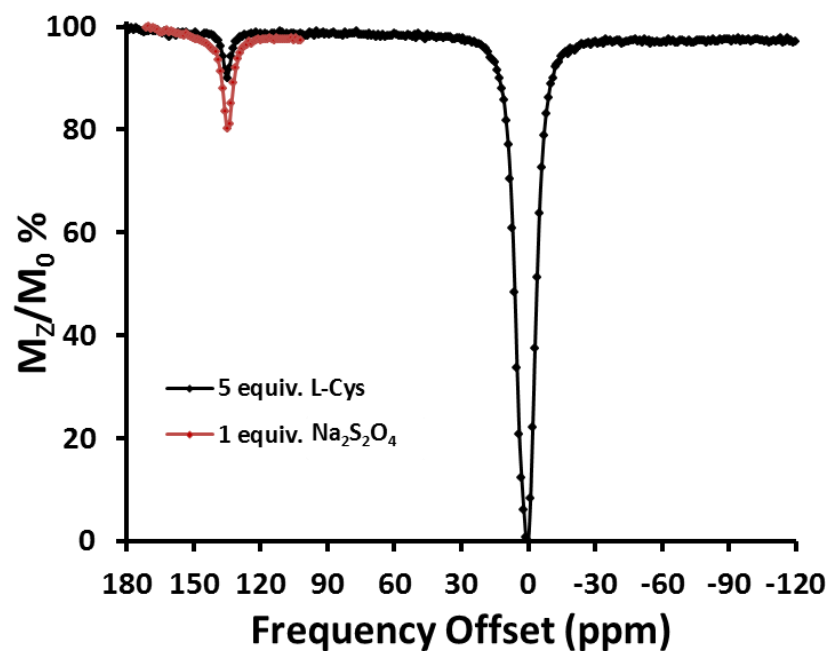
Figure S9. CEST spectrum upon reduction of 9.0 mM $[Co(TPT)]^{2+}$ with 1.0 equiv. $Na_2S_2O_4$ and 5.0 equiv. of L-cysteine, respectively. CEST spectra recorded at 11.7 T of a solution containing 200 mM NaCl, 40.0 mM HEPES pH 7.0, 37 ^{o}C. RF presaturation applied for 3 seconds, $B_1 =$ 24 μT at 37 °C. The large peak arises from direct irradiation of water protons, set to 0 ppm.
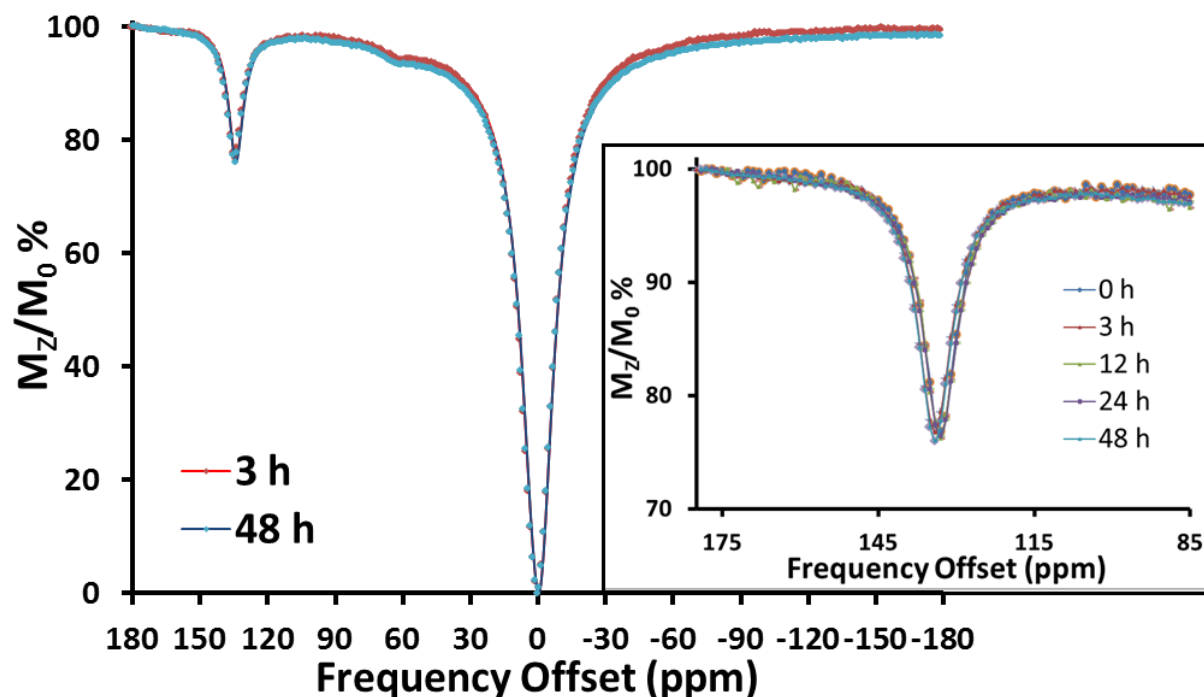
Figure S10. CEST spectrum of 8 mM $[Co(TPT)]^{2+}$ in rabbit serum at pH 6.95 and 37 °C under argon atmosphere. A lower intensity second CEST peak at +62 ppm was observed in serum which was absent in buffer. Insert shows that the major CEST peak is at +133 ppm in serum, slightly shifted from that in buffered solutions containing 40 mM HEPES, 200 mM NaCl. The CEST spectrum in serum did not change over a period of 48 h at 37 °C under inert atmosphere.

A

B
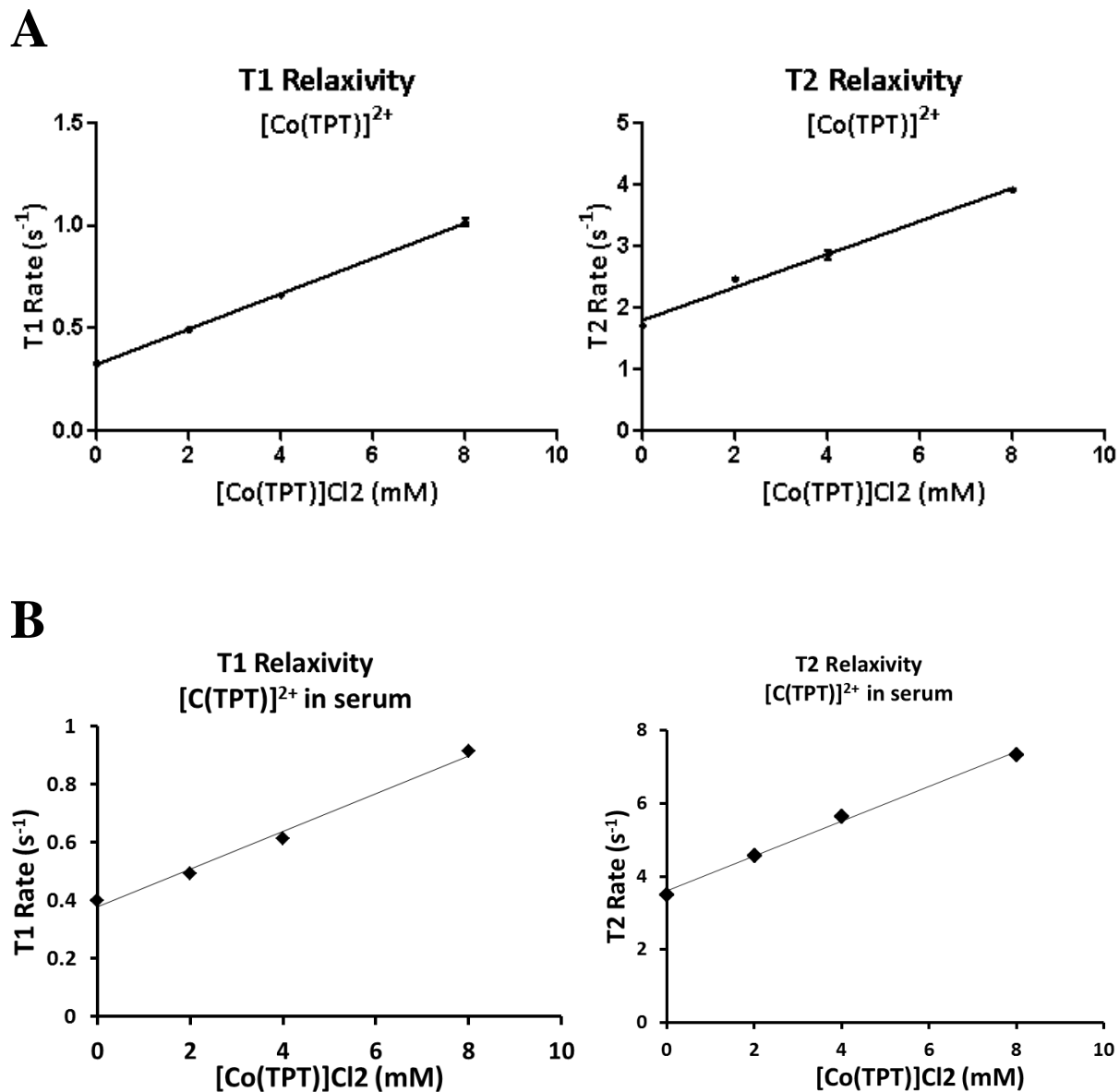
Figure S11. (A) Plots of T_1 (left) and T_2 (right) relaxation rate constants as a function of $[Co(TPT)]^{2+}$ concentration. T_1 and T_2 relaxivities were determined from slopes as 0.093 and 0.500 $(mM \cdot s)^{-1}$, respectively. Samples contained 40.0 mM HEPES buffer, pH 7.0, 200 mM NaCl. (B) Plots of T_1 (left) and T_2 (right) relaxation rate constants as a function of $[Co(TPT)]^{2+}$ concentration in rabbit serum. T_1 and T_2 relaxivities were determined from slopes as 0.065 and 0.478 $(mM \cdot s)^{-1}$, respectively.
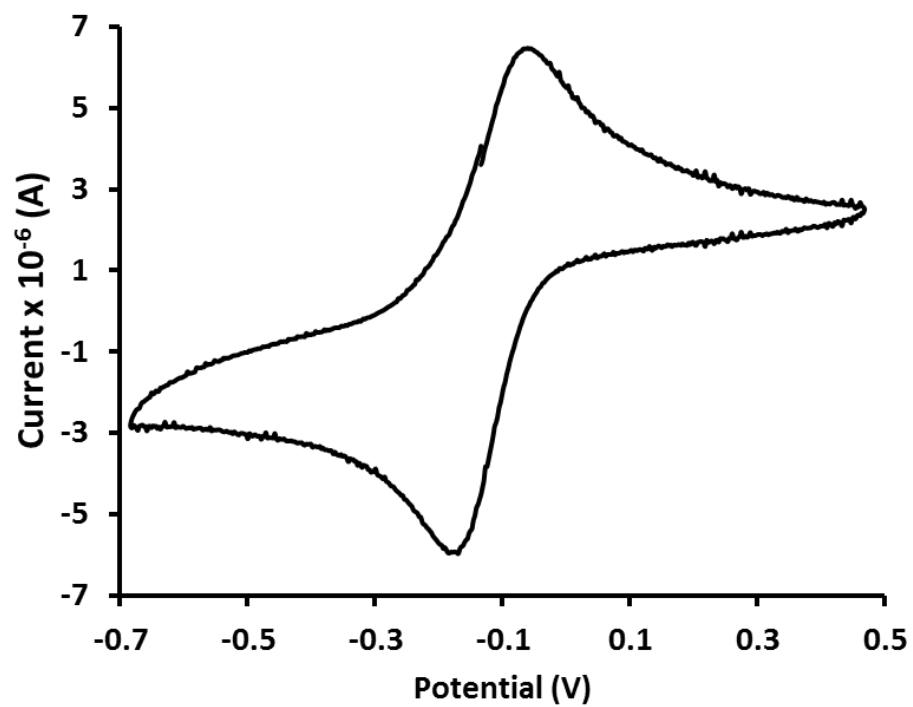
Figure S12. Cyclic voltammogram of argon-saturated aqueous solution of 1.7 mM [Co(TPT)]$^{2+}$ containing 1.00 M KCl, pH 6.0. A scan rate of 50 mV/s was used. Potentials are reported vs. NHE.
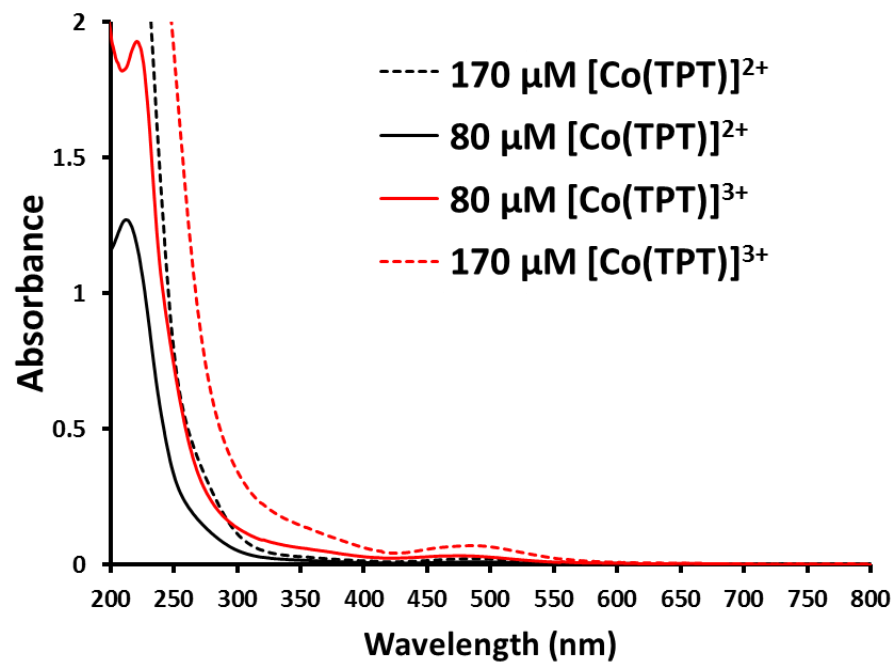
Figure S13. UV-vis spectra of $[Co(TPT)]^{2+}$ and $[Co(TPT)]^{3+}$ in 100 mM NaCl, 20.0 mM HEPES, pH 7.0. Spectrum of $[Co(TPT)]^{3+}$ has an additional red-shifted band with the maximum centered at $\lambda = 485$ nm.
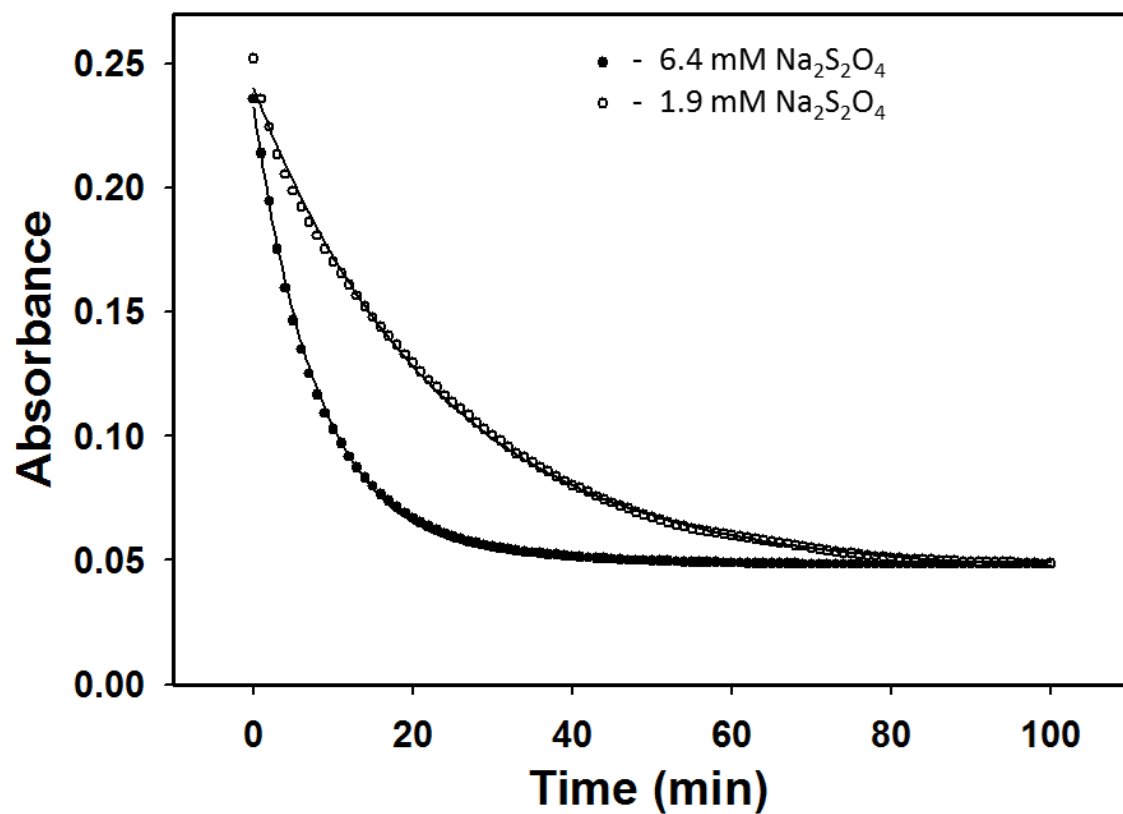
Figure S14. Determination of the pseudo-first order rate constants following the absorbance decay of 0.60 mM $[Co(TPT)]^{3+}$ in the presence of 1.90 mM and 6.40 mM $Na_2S_2O_4$ containing 0.20 M NaCl and 40.0 mM HEPES, pH 7.0. Solutions were purged with argon prior to mixing, and the samples were kept under inert atmosphere. Solid lines represent the fit of the data to a single exponential decay.
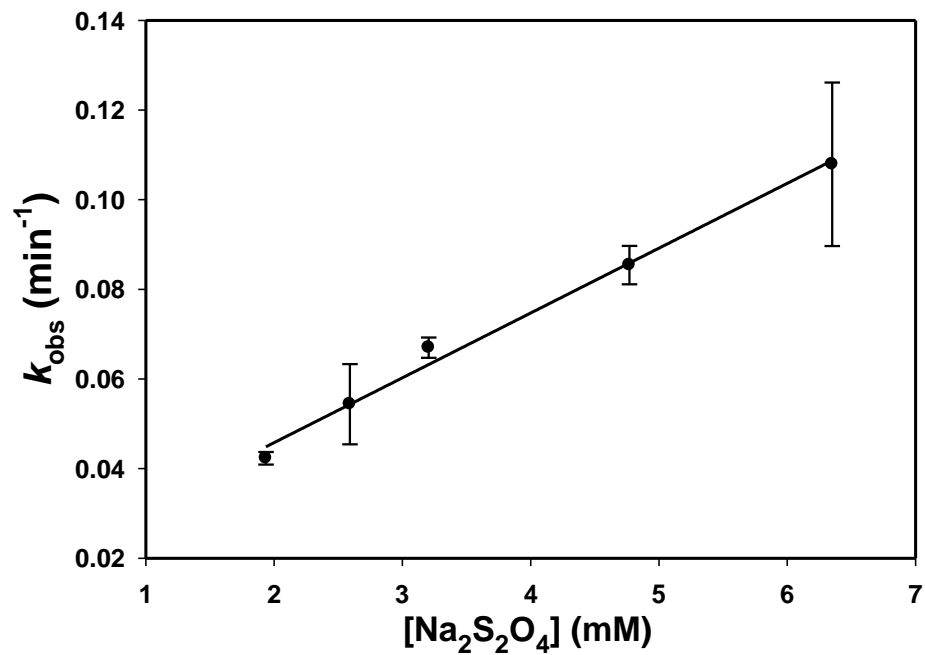
Figure S15. Dependence of the observed pseudo-first order rate constants for the reduction of 0.60 mM $[Co(TPT)]^{3+}$ on the $Na_2S_2O_4$ concentration at 200 mM NaCl, 40.0 mM HEPES, pH 7.0, 37 $^{\circ}$C. The linear fit of the data (solid line) gives a bimolecular rate constant $k_{bi} = 0.24$ $M^{-1}s^{-1}$.
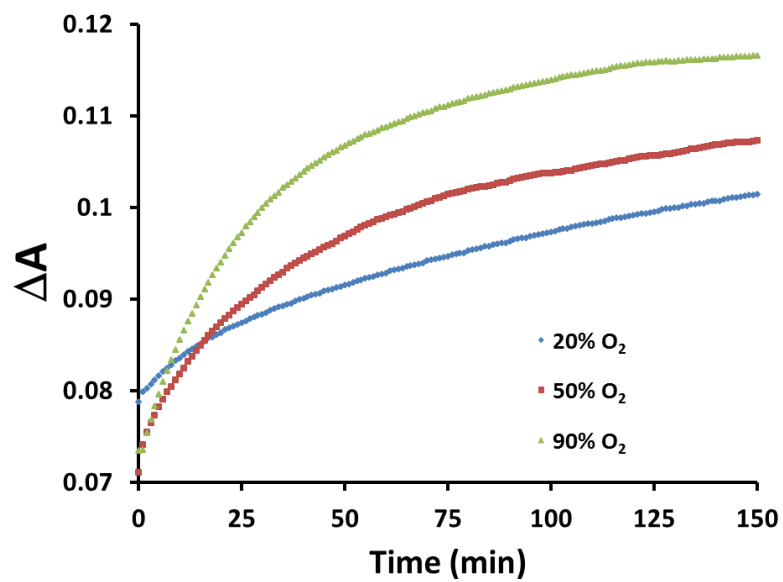
Figure S16. Single-exponential kinetic traces under pseudo-first order reaction conditions for 70 μM [Co(TPT)]$^{2+}$ oxidized with N$_2$/O$_2$ mixtures containing 20%, 50%, and 90% O$_2$, respectively, at 25 $^{\circ}$C. Solutions contained 200 mM NaCl and 40.0 mM HEPES, pH 7.1.
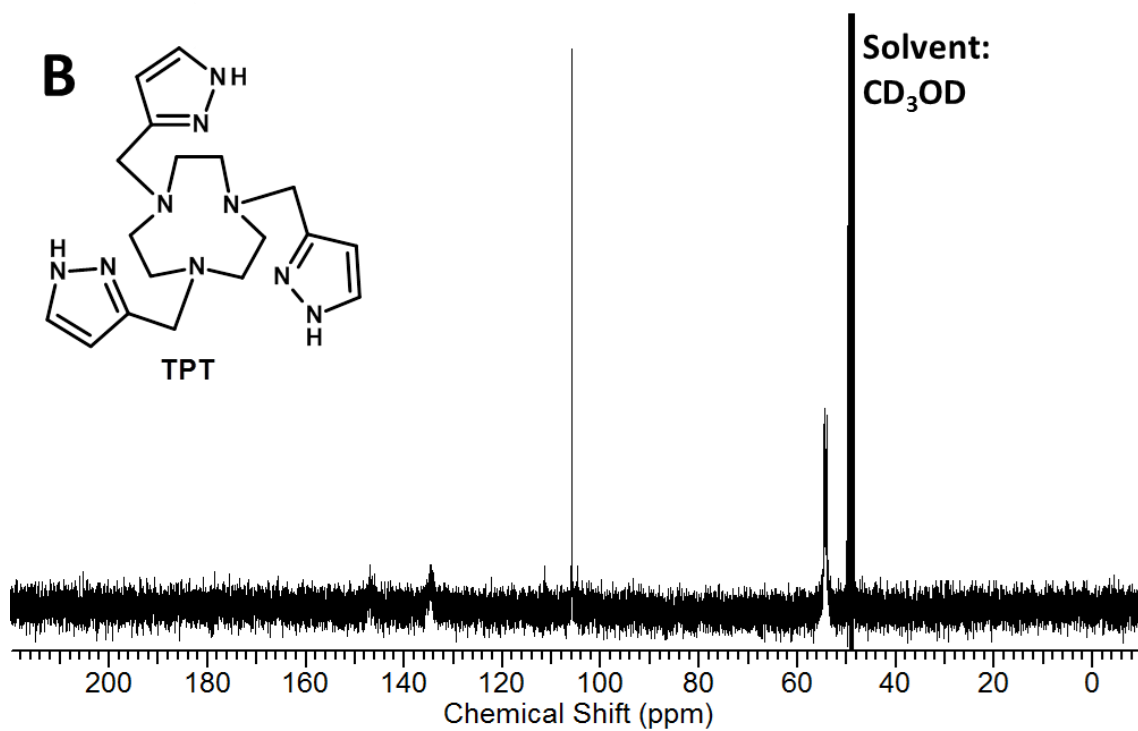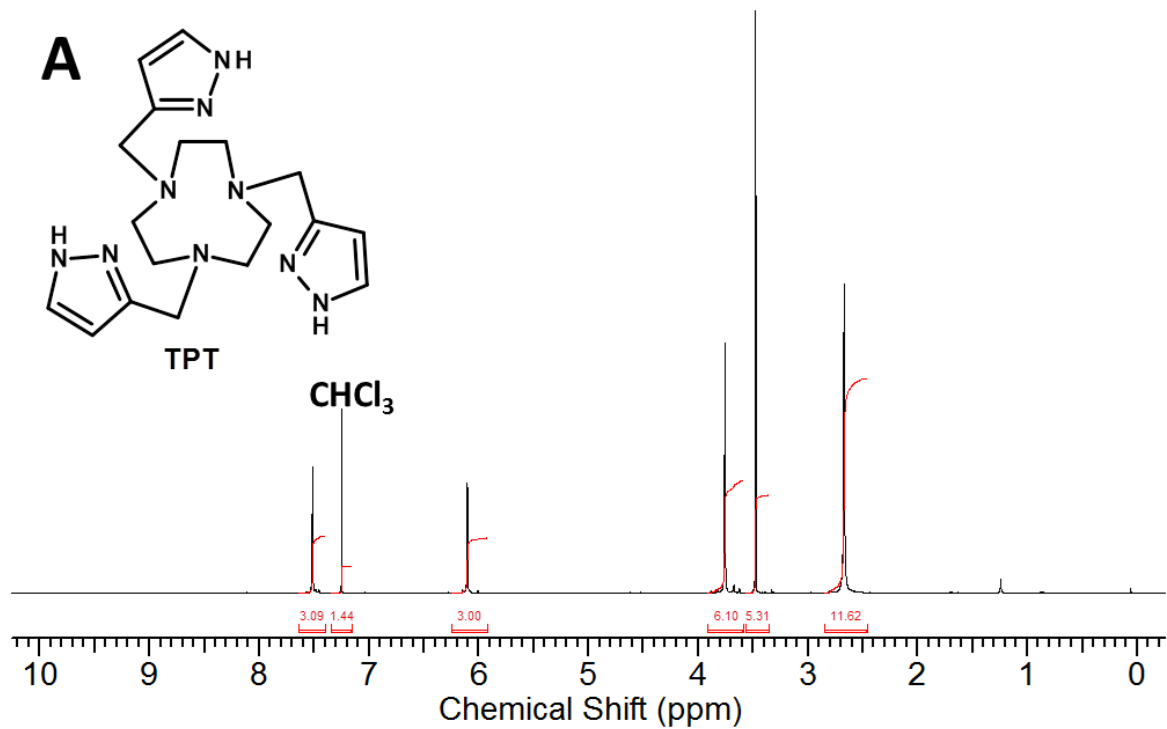
Figure S17. ^{1}H NMR spectrum of TPT ligand in CDCl$_3$ and ^{13}C NMR spectrum of TPT in CD$_3$OD.
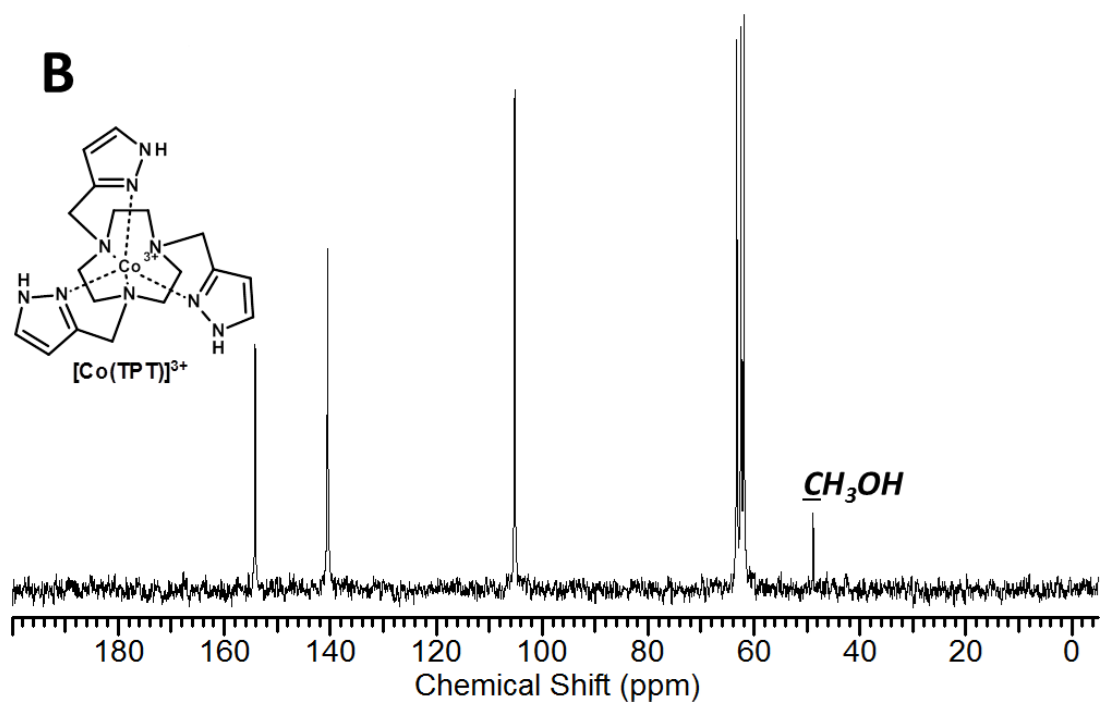
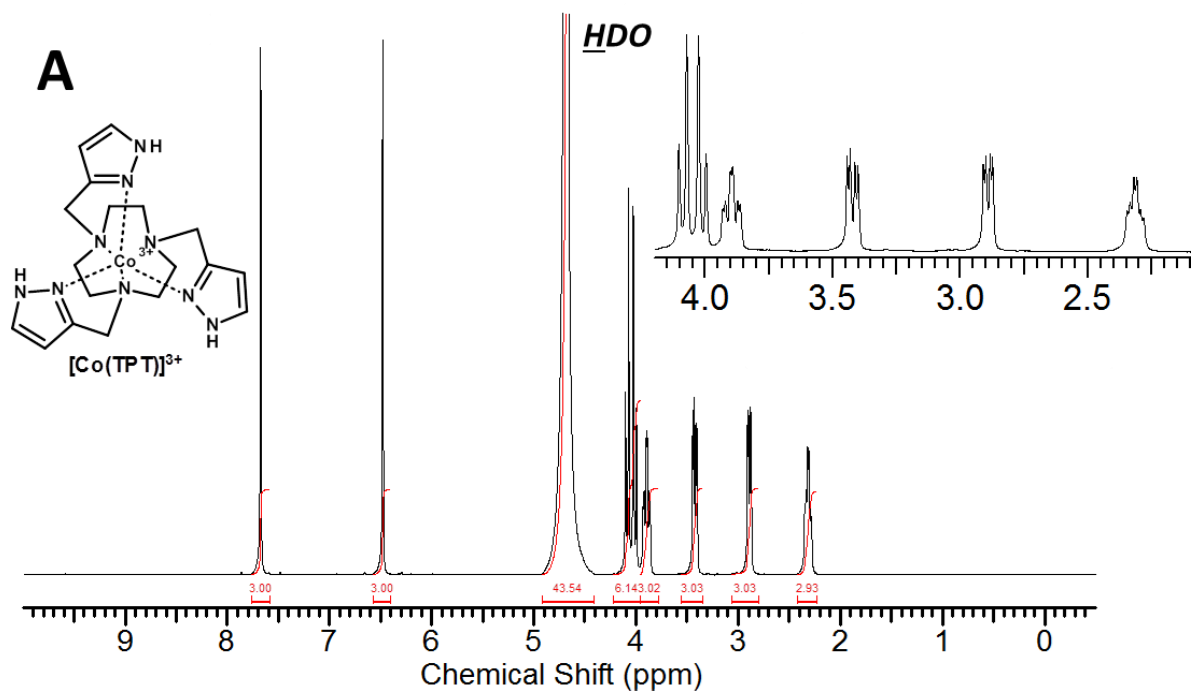**Figure S18.** ^{1}H NMR (A) and ^{13}C NMR (B) spectra of [Co(TPT)]$^{3+}$ in D$_2$O, pD 7.0. Methanol was used for ^{13}C NMR reference.

References

(1) Evans, D. F. *J. Chem. Soc*. **1959**, 2003.

(2) Dixon, W. T.; Ren, J.; Lubag, A. J. M.; Ratnakar, J.; Vinogradov, E.; Hancu, I.; Lenkinski, R.; Sherry, A. D. *Magn. Reson. Med*. **2010**, *63*, 625.

(3) Cole, E.; Copley, R. C. B.; Howard, J. A. K.; Parker, D.; Ferguson, G.; Gallagher, J. F.; Kaitner, B.; Harrison, A.; Royle, L. *J. Chem. Soc. Dalton Trans*. **1994**, 1619.